Advanced CNN-Based Image Denoising Techniques for Digital Forensics Applications

H. S. Annapurna
Department of Information Science and Engineering, Sri Siddhartha Institute of Technology, Sri Siddhartha Academy of Higher Education, Tumakuru, India
annapoornahs@ssit.edu.in (corresponding author)

K. Mala
Department of Information Science and Engineering, Channabasaveshwara Institute of Technology, Tumakuru, India | Visvesvaraya Technological University, Belagavi, India
mala.k@cittumkur.org

Gousia Thahniyath
Department of Computer Science and Engineering, Dayananda Sagar University, Bengaluru, India
gusia-cse@du.edu.in

V. C. Rudramurthy
Department of Computer Science and Engineering, B.M.S. College of Engineering, Bengaluru, India
rudramurtyvc.ise@bmsce.ac.in

Mohan T. G. Kumar
Department of Information Science and Engineering, Nitte Meenakshi Institute of Technology (NMIT), Nitte (Deemed to be University), Visvesvaraya Technological University, Belagavi, India
mohankumar.tg@nmit.ac.in

G. K. Shwetha
Department of Computer Science and Engineering, ATME College of Engineering, Mysuru, India
gk.shweta@gmail.com

Received: 17 February 2026 | Revised: 22 March 2026 and 2 April 2026 | Accepted: 3 April 2026

 DOI: https://doi.org/10.48084/etasr.18234

ABSTRACT

In digital forensics, image denoising is essential because the caliber and clarity of visual evidence have a strong influence on the results of investigations and court cases. Gaussian noise, salt-and-pepper noise, Poisson noise, and speckle noise are just a few of the noise types that are frequently introduced during the collection, transmission, or storage of forensic photographs. Although computationally efficient, traditional denoising techniques, such as median filtering and bilateral filtering, frequently lose edge information and small features that are essential for forensic investigation. This study suggests a sophisticated Convolutional Neural Network (CNN) architecture that includes adversarial training elements, multi-scale processing, residual learning, and attention processes, especially tailored for forensic picture denoising. The proposed approach successfully reduces noise across a variety of noise kinds and intensity levels while preserving evidentiary integrity, addressing the difficulties of forensic imaging. The superiority of the suggested method is demonstrated by extensive experimental validation on standard datasets such as MNIST, BSD68, and Set12, yielding Structural Similarity Index Measure (SSIM) scores of 0.92 and Peak Signal-to-Noise Ratio (PSNR) improvements of 10.2 dB over noisy inputs, significantly outperforming traditional methods. With an average inference time of 0.02 s per image on typical GPU hardware, the model demonstrates computational efficiency and is appropriate for real-time forensic applications. A comparison with cutting-edge methods confirms the suggested approach's resilience and capacity for generalization in a variety of forensic contexts.

Keywords-image denoising; digital forensics; convolutional neural networks; residual learning; attention mechanisms; deep learning; image quality enhancement; forensic evidence analysis

I. INTRODUCTION

Digital forensics plays a vital role in modern law enforcement and judicial processes, with digital images serving as key sources of evidentiary information. Image quality is critical in this context, as noise degrades visual evidence and affects analysis accuracy [1]. The rapid growth of imaging devices and surveillance systems has increased the availability of forensic images, but their quality is often degraded by noise arising from sensor limitations, low-light conditions, compression, transmission errors, and storage effects [2]. Such degradation can obscure critical visual details and introduce ambiguity in forensic interpretation, potentially affecting the reliability of evidence and legal outcomes. Unlike general image enhancement tasks, forensic image processing demands high reconstruction fidelity, where deep residual learning architectures have demonstrated strong capacity to preserve fine structural details essential for reliable evidence analysis [3, 4].

Traditional image denoising techniques, including spatial filters and transform-domain techniques, provide basic noise reduction but frequently compromise edge information and fine details, limiting their effectiveness in sensitive forensic image analysis tasks, while recent surveys highlight the growing adoption of deep learning to address such limitations in image forensics [5]. Although non-local and sparsity-based approaches improve texture preservation, their effectiveness remains limited under complex and heterogeneous noise conditions commonly encountered in forensic imagery. Denoising performance has been significantly enhanced by data-driven modeling of noise characteristics, made feasible by the development of deep learning, particularly Convolutional Neural Networks (CNNs) with residual learning [4]. Recent developments incorporating generative adversarial networks, attention mechanisms, multi-scale feature extraction, and adversarial learning have further enhanced detail preservation and perceptual quality across varying noise levels [6].

Despite these advances, existing deep CNN denoising methods face training challenges related to performance saturation and limited generalizability across diverse noise conditions [7]. Furthermore, CNN-based denoising autoencoders, while effective at noise suppression, may inadvertently blur fine structural features critical for downstream recognition and analysis tasks [8]. The interplay between denoising preprocessing and downstream CNN-based recognition performance further highlights the need for lightweight and efficient denoising strategies suitable for embedded and resource-constrained deployment scenarios [9]. To overcome these obstacles, this research focuses on a specialized CNN-based denoising framework that integrates residual learning, attention-driven feature prioritization, multi-scale processing, and adversarial components to achieve robust noise reduction while preserving forensic detail and maintaining practical computational efficiency [10].

II. PROPOSED METHOD

The proposed CNN is designed as a modular denoising framework optimized for forensic image analysis, where noise suppression must be achieved without compromising evidentiary details [11]. The architecture integrates four tightly coupled components: a Multi-Scale Feature Extraction module, a Residual Learning framework, an Attention Mechanism module, and an Adversarial Refinement component [11]. This structured design enables effective feature learning across varying noise distributions while maintaining end-to-end trainability and adaptability to diverse forensic imaging conditions [12]. In addition, an encoder-decoder configuration with skip connections is employed to balance hierarchical feature abstraction and spatial detail preservation [13]. With the use of encoder feature maps, the encoder gradually downsamples the input to provide contextual representations, while the decoder uses transposed convolutions to restore spatial resolution [14]. This architecture ensures that during denoising, both fine-grained forensic features and global structure are preserved, while remaining computationally efficient for deployment on resource-constrained platforms [15].

A. Dataset

The model was trained and evaluated on standard benchmark datasets, namely MNIST [16, 17], BSD68 [18, 19], and Set12 [20, 21], which collectively provide diversity in image structure, content, and complexity. MNIST provides grayscale digit images suitable for assessing structural preservation, BSD68 offers a broad range of natural image textures and scene types, and Set12 provides a compact but representative set for denoising benchmarking. Both grayscale and color images were used and resized to a uniform spatial resolution to ensure consistency during training. Clean images from these datasets were synthetically degraded using Gaussian, salt-and-pepper, Poisson, and speckle noise at varying intensity levels (σ = 15, 25, 50) to simulate realistic forensic noise conditions, following established evaluation protocols in the denoising literature [13, 22]. The dataset was divided into training, validation, and testing subsets using a 70:15:15 split with no overlap. To improve robustness and reduce overfitting, data augmentation techniques including rotation, flipping, and random cropping were applied. Ground-truth clean images were retained for objective and perceptual performance evaluation under both supervised and adversarial training settings [23]. These benchmark datasets, while not exclusively forensic in origin, are widely used in the denoising literature and provide a standardized and reproducible basis for comparative evaluation of the proposed framework.

B. Multi-Scale Feature Extraction

To address noise present at different spatial frequencies, the Multi-Scale Feature Extraction module applies parallel convolutional filters with kernel sizes of 3×3, 5×5, and 7×7 [11]. These kernels capture complementary information, ranging from fine textures to broader contextual structures commonly observed in forensic imagery. The extracted feature

maps are concatenated and fused using a 1×1 convolution, enabling dimensionality reduction and effective integration of multi-scale information.

The feature fusion process is defined as:

$$F_{fused} = \sigma(W_{1\times1} * [F_{3\times3} \oplus F_{5\times5} \oplus F_{7\times7}]) \quad (1)$$

where F_{fused} denotes the aggregated feature representation, $W_{1\times1}$ represents the fusion weights, $\oplus$ indicates concatenation, and σ is the activation function. Furthermore, dilated convolutions with dilation rates of 1, 2, and 4 are incorporated to expand the receptive field without increasing the number of parameters, enabling the network to capture long-range spatial dependencies essential for contextual noise suppression [15].

C. Residual Learning Framework

Instead of immediately reconstructing the clean image, the network is trained to estimate the noise component in the denoising job using a residual learning technique. This simplifies optimization and accelerates convergence by exploiting the structured nature of noise patterns. The expected noise is subtracted from the noisy input image to obtain the denoised output. The residual formulation is expressed as:

$$\hat{I}_{clean} = I_{noisy} - R(I_{noisy}; \Theta) \quad (2)$$

where $R(\cdot;\Theta)$ represents the residual mapping function parameterized by Θ. Residual blocks with identity skip connections are embedded throughout the network to facilitate gradient flow and stabilize deep network training. This dual-level residual strategy—at both image and feature levels—enhances robustness and denoising accuracy.

D. Attention Mechanism Integration

An attention mechanism is incorporated to deliberately highlight forensically significant portions while squelching less informative ones. Channel attention and spatial attention are applied sequentially to recalibrate feature responses. Channel attention assigns adaptive weights to feature channels based on global context, while spatial attention highlights critical regions such as edges and texture boundaries. The channel attention operation is given by:

$$A_c = \sigma(MLP(GAP(F)) + MLP(GMP(F))) \quad (3)$$

where A_c denotes channel attention weights, GAP and GMP are global pooling operations, and MLP represents a shared multi-layer perception. These attention maps are applied multiplicatively to refine feature representations, enabling precise noise suppression without degrading essential forensic information.

E. Adversarial Refinement and Training Strategy

To further enhance perceptual fidelity, an adversarial training component based on a PatchGAN discriminator is employed. The discriminator distinguishes denoised outputs from clean reference images, encouraging realistic texture reconstruction and natural image statistics. The generator is optimized using a composite loss function:

$$\mathcal{L}_{total} = \lambda_1\mathcal{L}_{L1} + \lambda_2\mathcal{L}_{perceptual} + \lambda_3\mathcal{L}_{adv} \quad (4)$$

where pixel-level accuracy, perceptual consistency, and adversarial realism are jointly enforced. The network is trained using the Adam optimizer with adaptive learning rate scheduling, supported by data augmentation and multi-noise training to ensure robustness across diverse forensic scenarios.

F. Network Architecture Illustration

Figure 1 presents the complete architecture of the proposed CNN-based denoising framework. The diagram illustrates the flow of information from the input noisy image through multi-scale feature extraction, residual learning with attention enhancement, and decoder reconstruction, followed by adversarial refinement. The final output is a denoised image that preserves critical forensic details while effectively suppressing noise. The architecture incorporates skip connections between corresponding encoder and decoder levels to preserve high-frequency spatial information necessary for forensic trace analysis. Feature normalization and adaptive loss optimization mechanisms are additionally incorporated to stabilize training and enhance reconstruction fidelity across varying noise distributions [23].

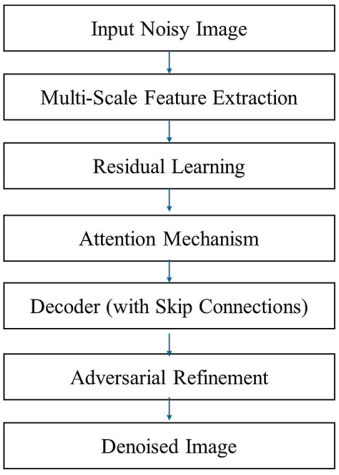

Fig. 1. Architecture of the proposed method.

III. RESULTS AND DISCUSSION

A. Experimental Setup

The proposed denoising framework was evaluated using standard benchmark datasets, namely MNIST, BSD68, and Set12, to ensure diversity in image structure and content. Gaussian noise was synthetically added at multiple noise levels (σ = 15, 25, 50) to simulate realistic degradation scenarios. An NVIDIA A100 GPU with 40 GB of RAM was used for model training, with a batch size of 16 and 100 epochs. Peak Signal-to-Noise Ratio (PSNR), Structural Similarity Index Measure (SSIM), and computational efficiency measures were used in the performance evaluation. In addition to quantitative assessment, convergence stability was monitored through validation loss trends to ensure consistent learning behavior across epochs. To confirm the statistical significance and generalization potential of the suggested model under various noise distributions, a comparison with baseline denoising techniques was also carried out.

B. Quantitative Performance Evaluation

Quantitative results demonstrate substantial improvements over noisy inputs across all datasets. On the MNIST test set, PSNR increased from 20.3 dB to 30.5 dB, while SSIM improved from 0.65 to 0.92, indicating effective noise suppression with strong structural preservation. Similar performance gains were observed on BSD68 and Set12 at higher noise levels, as summarized in Tables I and II.

Table I offers a PSNR comparison, demonstrating consistent enhancement in signal reconstruction quality after denoising across all evaluated datasets. The substantial gain in decibel values indicates effective reduction of additive noise while maintaining intensity fidelity, particularly under higher noise variances such as $\sigma = 50$.

TABLE I. PEAK SIGNAL-TO-NOISE RATIO (PSNR) COMPARISON

Dataset	Noisy Image PSNR	Denoised PSNR
MNIST test set	20.3 dB	30.5 dB
BSD68 (σ = 25)	18.6 dB	29.2 dB
Set12 (σ = 50)	14.2 dB	25.8 dB

TABLE II. STRUCTURAL SIMILARITY INDEX (SSIM) COMPARISON

Dataset	Noisy Image SSIM	Denoised SSIM
MNIST sest set	0.65	0.92
BSD68 (σ =25)	0.58	0.89
Set12 (σ = 50)	0.42	0.84

Table II shows the SSIM comparison. The SSIM improvements reflect significant preservation of structural and perceptual image characteristics following the denoising process. Higher SSIM scores across MNIST, BSD68, and Set12 confirm that the proposed framework maintains edge integrity and textural consistency even under severe noise conditions. These results confirm the robustness of the proposed model across diverse image types and noise intensities, which is essential for forensic applications.

C. Comparative Analysis with Existing Methods

The proposed approach was compared with state-of-the-art denoising techniques, including DnCNN, FFDNet, bilateral filtering, and Non-Local Means, using the BSD68 dataset at σ = 25. As reported in Table III, the proposed method achieved the highest PSNR (29.2 dB) and SSIM (0.89), outperforming all competing techniques. This performance is attributed to the combined use of multi-scale feature extraction, residual learning, attention mechanisms, and adversarial refinement, aligning with recent deep learning-based denoising studies.

TABLE III. COMPARISON WITH EXISTING METHODS

Method	PSNR (dB)	SSIM
Proposed method	29.2	0.89
DnCNN	28.8	0.86
FFDNet	28.5	0.85
Bilateral Filter	26.3	0.78
Non-Local Means	27.1	0.81

A deeper analysis of the comparative results reveals several important distinctions between the proposed method and existing approaches. DnCNN, which relies solely on residual learning without attention or multi-scale processing, achieves a PSNR of 28.8 dB and SSIM of 0.86 on BSD68 at σ = 25, demonstrating the baseline strength of residual CNN architectures but falling short in perceptual fidelity under complex noise distributions. FFDNet, designed for spatially variant noise via a noise level map input, achieves 28.5 dB PSNR and 0.85 SSIM. Although FFDNet offers flexibility in handling different noise levels, its performance on fixed-variance benchmarks is slightly lower than DnCNN due to the additional parameterization burden. The proposed method surpasses both DnCNN and FFDNet by 0.4 dB and 0.7 dB PSNR and 0.03 and 0.04 SSIM, respectively, at this noise level. These gains are attributable to the joint integration of multi-scale feature extraction, channel-spatial attention, and adversarial refinement, which enable the proposed model to better capture and suppress noise while recovering fine-grained detail. Traditional methods, namely bilateral filtering and Non-Local Means, perform considerably below the deep learning approaches (26.3 dB and 27.1 dB PSNR, respectively), confirming the well-established limitation of handcrafted filters in modeling complex noise statistics, particularly relevant in forensic imaging contexts where evidentiary fine structure must be preserved. These results collectively affirm that the integration of complementary architectural components provides measurable and consistent advantages over both classical and modern deep learning denoising baselines.

D. Ablation Study

An ablation study was carried out to evaluate each architectural component's contribution. The results presented in Table IV show that removing residual connections led to the most significant degradation in performance (28.1 dB PSNR, 0.85 SSIM), highlighting their critical role in stable training and noise modeling. Excluding attention mechanisms or multi-scale processing also reduced performance, confirming their importance in selective feature enhancement and multi-resolution representation. The absence of adversarial training had a comparatively smaller impact, suggesting its primary contribution is perceptual refinement rather than core denoising accuracy.

TABLE IV. ABLATION STUDY RESULTS

Model variant	PSNR (dB)	SSIM
Full Model (Proposed)	30.5	0.92
Without Residual Connections	28.1	0.85
Without Attention Mechanisms	29.3	0.88
Without Multi-Scale Processing	29.6	0.89
Without Adversarial Training	30.1	0.90

E. Visual Quality Assessment

Qualitative analysis further validates the quantitative results. Figure 2 demonstrates effective noise removal with clear preservation of digit structures. The reconstructed outputs show smooth background regions while retaining sharp stroke continuity and well-defined boundaries, indicating that the model successfully distinguishes noise components from meaningful structural information. This demonstrates that

precise spatial restoration is supported by the learnt hierarchical feature representations. Furthermore, Figure 3 demonstrates how the model may preserve tiny details without over-smoothing or adding artifacts. The noisy image (left) and the denoised image (right) comparison in Figure 4 shows significant noise reduction while maintaining structural integrity and significant image features. Visual assessment across more complex datasets such as BSD68 and Set12 further demonstrates consistent restoration of natural textures, object contours, and gradient variations under different noise intensities. The absence of halo artifacts, ringing effects, or artificial sharpening confirms stable reconstruction behavior, which is essential in forensic contexts where preservation of evidential features and interpretability must remain uncompromised.

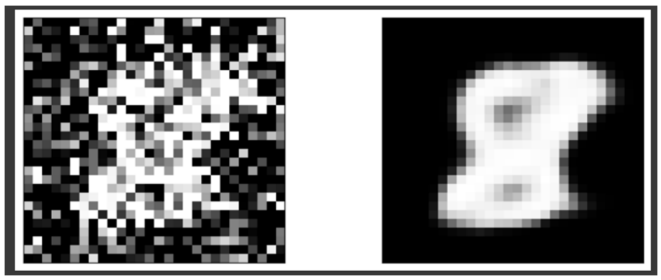

Fig. 2. Visual comparison of noisy input (left) and denoised output (right) on the MNIST dataset.

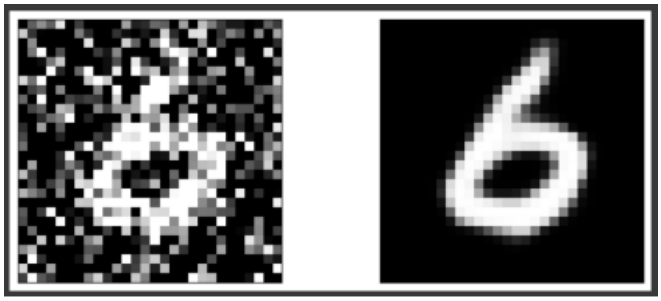

Fig. 3. Additional example demonstrating edge preservation and texture recovery.

Fig. 4. Image with noise (left) and without noise (right).

F. Computational Efficiency Analysis

Computational efficiency was evaluated to assess practical applicability. The proposed model achieved an average inference time of 0.02 s per MNIST-sized image and 0.18 s for 256×256 images on an NVIDIA A100 GPU, with an overall memory footprint of approximately 850 MB. These results support real-time and offline forensic workflows, including deployment on edge devices with limited computational resources. The balance between high denoising accuracy and computational efficiency makes the proposed framework suitable for operational forensic imaging systems.

IV. CONCLUSION

The proposed CNN-based denoising framework for digital forensics integrates residual connections, multi-scale feature extraction, attention mechanisms, and adversarial refinement to improve image quality while preserving evidentiary details. Experimental evaluation shows that the model outperforms conventional and recent deep learning denoising approaches, achieving 30.5 dB PSNR and 0.92 SSIM on benchmark datasets. Residual learning supports stable optimization in deep layers, attention modules enhance important forensic regions, and multi-scale representations improve robustness across varying noise patterns, while adversarial learning contributes to perceptual quality with acceptable computational cost.

However, several limitations should be noted. The current evaluation relies on synthetically generated noise rather than real acquisition noise, which may not fully represent practical forensic environments such as low-light surveillance systems or compressed evidence images. In addition, the benchmark datasets used—MNIST, BSD68, and Set12—are standard denoising datasets but are not specifically designed for forensic applications and do not include evidentiary image categories such as fingerprints, questioned documents, or ballistic imagery. The adversarial component also introduces training sensitivity, and computational results obtained on high-end GPU hardware may not directly reflect deployment performance in field-based forensic systems.

Future work should focus on developing forensic-specific benchmark datasets containing authentic noisy evidence images and real-world acquisition conditions. Extending the framework toward real-noise estimation, blind denoising, and hybrid CNN-Transformer architectures may improve generalization and spatial detail recovery in complex forensic imagery. Beyond PSNR and SSIM, future evaluation should include forensic relevance metrics such as fingerprint identification accuracy and document character recovery, ensuring that denoising performance remains aligned with evidentiary reliability requirements in operational forensic practice.

DECLARATION OF COMPETING INTERESTS

Not applicable to this work.

ACKNOWLEDGMENT

The authors gratefully acknowledge the financial assistance provided by the Vision Group on Science and Technology (VGST), Department of Electronics, Information Technology, Biotechnology and Science & Technology", Government of Karnataka, under the K-FIST Level-1 scheme

(Grant No. VGST/K-FIST(L1)/GRD-1144) for supporting this research work.

DATA AVAILABILITY

The datasets used in this study are publicly available in [17, 19, 21] and were utilized in accordance with their respective licensing and citation requirements.

REFERENCES

[1] S. Rani, Y. Chabrra, and K. Malik, "An Improved Denoising Algorithm for Removing Noise in Color Images," *Engineering, Technology & Applied Science Research*, vol. 12, no. 3, pp. 8738–8744, June 2022, https://doi.org/10.48084/etasr.4952.

[2] A. E. Ilesanmi and T. O. Ilesanmi, "Methods for image denoising using convolutional neural network: a review," *Complex & Intelligent Systems*, vol. 7, no. 5, pp. 2179–2198, Oct. 2021, https://doi.org/10.1007/s40747-021-00428-4.

[3] M. Shafiq and Z. Gu, "Deep Residual Learning for Image Recognition: A Survey," *Applied Sciences*, vol. 12, no. 18, Sept. 2022, Art. no. 8972, https://doi.org/10.3390/app12188972.

[4] C. Tian, L. Fei, W. Zheng, Y. Xu, W. Zuo, and C. W. Lin, "Deep learning on image denoising: An overview," *Neural Networks*, vol. 131, pp. 251–275, Nov. 2020, https://doi.org/10.1016/j.neunet.2020.07.025.

[5] M. Zanardelli, F. Guerrini, R. Leonardi, and N. Adami, "Image forgery detection: a survey of recent deep-learning approaches," *Multimedia Tools and Applications*, vol. 82, no. 12, pp. 17521–17566, May 2023, https://doi.org/10.1007/s11042-022-13797-w.

[6] I. Goodfellow *et al.*, "Generative adversarial networks," *Communications of the ACM*, vol. 63, no. 11, pp. 139–144, Oct. 2020, https://doi.org/10.1145/3422622.

[7] C. Tian, Y. Xu, and W. Zuo, "Image denoising using deep CNN with batch renormalization," *Neural Networks*, vol. 121, pp. 461–473, Jan. 2020, https://doi.org/10.1016/j.neunet.2019.08.022.

[8] Y. Farooq and S. Savaş, "Noise Removal from the Image Using Convolutional Neural Networks-Based Denoising Auto Encoder," *Journal of Emerging Computer Technologies*, vol. 3, no. 1, pp. 21–28, Mar. 2024, https://doi.org/10.57020/ject.1390428.

[9] R. Kaur, G. Karmakar, and M. Imran, "Impact of Traditional and Embedded Image Denoising on CNN-Based Deep Learning," *Applied Sciences*, vol. 13, no. 20, Oct. 2023, Art. no. 11560, https://doi.org/10.3390/app132011560.

[10] B. Goyal, A. Dogra, S. Agrawal, B. S. Sohi, and A. Sharma, "Image denoising review: From classical to state-of-the-art approaches," *Information Fusion*, vol. 55, pp. 220–244, Mar. 2020, https://doi.org/10.1016/j.inffus.2019.09.003.

[11] S. Zhang, C. Liu, Y. Zhang, S. Liu, and X. Wang, "Multi-Scale Feature Learning Convolutional Neural Network for Image Denoising," *Sensors*, vol. 23, no. 18, Sept. 2023, Art. no. 7713, https://doi.org/10.3390/s23187713.

[12] S. Woo, J. Park, J. Y. Lee, and I. S. Kweon, "CBAM: Convolutional Block Attention Module," in *Computer Vision – ECCV 2018*, vol. 11211, V. Ferrari, M. Hebert, C. Sminchisescu, and Y. Weiss, Eds. Springer International Publishing, 2018, pp. 3–19.

[13] A. M. Ali, B. Benjdira, A. Koubaa, W. El-Shafai, Z. Khan, and W. Boulila, "Vision Transformers in Image Restoration: A Survey," *Sensors*, vol. 23, no. 5, Feb. 2023, Art. no. 2385, https://doi.org/10.3390/s23052385.

[14] Y. Cui, M. Shi, and J. Jiang, "Multi-Scale Detail–Noise Complementary Learning for Image Denoising," *Applied Sciences*, vol. 14, no. 16, Aug. 2024, Art. no. 7044, https://doi.org/10.3390/app14167044.

[15] M. T. Duong, B. T. Nguyen Thi, S. Lee, and M. C. Hong, "Multi-Branch Network for Color Image Denoising Using Dilated Convolution and Attention Mechanisms," *Sensors*, vol. 24, no. 11, June 2024, Art. no. 3608, https://doi.org/10.3390/s24113608.

[16] Y. Lecun, L. Bottou, Y. Bengio, and P. Haffner, "Gradient-based learning applied to document recognition," *Proceedings of the IEEE*, vol. 86, no. 11, pp. 2278–2324, Nov. 1998, https://doi.org/10.1109/5.726791.

[17] "MNIST Database of Handwritten Digits." UCI Machine Learning Repository, 1998, https://doi.org/10.24432/C53K8Q.

[18] D. Martin, C. Fowlkes, D. Tal, and J. Malik, "A database of human segmented natural images and its application to evaluating segmentation algorithms and measuring ecological statistics," in *Proceedings Eighth IEEE International Conference on Computer Vision. ICCV 2001*, 2001, vol. 2, pp. 416–423, https://doi.org/10.1109/ICCV.2001.937655.

[19] "clausmichele/CBSD68-dataset." [Online]. Available: https://github.com/clausmichele/CBSD68-dataset.

[20] K. Zhang, W. Zuo, Y. Chen, D. Meng, and L. Zhang, "Beyond a Gaussian Denoiser: Residual Learning of Deep CNN for Image Denoising," *IEEE Transactions on Image Processing*, vol. 26, no. 7, pp. 3142–3155, July 2017, https://doi.org/10.1109/TIP.2017.2662206.

[21] "datasets/Set12," *GitLab*. https://plmlab.math.cnrs.fr/matias.tassano/dct-cnn/-/tree/master/datasets/Set12?ref_type=heads.

[22] H. Liu, Z. Li, S. Lin, and L. Cheng, "A Residual UNet Denoising Network Based on Multi-Scale Feature Extraction and Attention-Guided Filter," *Sensors*, vol. 23, no. 16, Aug. 2023, Art. no. 7044, https://doi.org/10.3390/s23167044.

[23] P. Isola, J. Y. Zhu, T. Zhou, and A. A. Efros, "Image-to-Image Translation with Conditional Adversarial Networks," in *2017 IEEE Conference on Computer Vision and Pattern Recognition (CVPR)*, July 2017, pp. 5967–5976, https://doi.org/10.1109/CVPR.2017.632.